Effect of Coarse Aggregates on FRP Strain Distribution in a FRP-to-Concrete Bonded Joint

Ya-Qi Li, Esmaeel Esmaeeli, Jian-Fei Chen, Wei Sha and Marios Soutsos
School of Natural and Built Environment, Queen's University Belfast, Belfast, UK

ABSTRACT

Advanced fibre-reinforced polymer (FRP) composites have been widely used for strengthening concrete structures. The bond behaviour between FRP and concrete plays the crucial role in this technique. Commonly the test of this bond behaviour is conducted using a single or double shear pull-off test of an FRP-to-concrete bonded joint, or similar bending tests. Such test setups are usually modelled as a two dimensional (2D) plane stress or plane strain structure. However, the test setup is in reality a three-dimensional (3D) structure due to many factors. One of the main factors is that the concrete behaviour is three dimensional because of the presence of coarse aggregates. Because of the random distribution of coarse aggregates in concrete, it may be expected that the non-uniformity of strain distribution is also random. Compared to concrete, mortar is a much more uniform material. In the research work presented in this paper, an experimental study is employed to investigate the strain distribution in the FRP in a bond test, where the FRP was bonded to either concrete or mortar. The results confirm that the presence of coarse aggregates in the concrete leads to much more variation in the FRP strain distribution.

INTRODUCTION

Fibre-reinforced polymer (FRP) has been widely investigated as well as used around the world for the strengthening of reinforced concrete (RC) structures. In FRP-strengthened RC structures, one of the main failure modes is the separation of FRP from concrete (debonding) [1]. This has led to extensive research, both experimentally and numerically, on the bond behaviour between FRP and concrete. In experimental studies, the debonding of FRP is typically investigated using the single-lap shear test of FRP–concrete bonded specimen, in which an FRP plate is bonded onto a concrete prism and subjected to a tensile force (e.g. [2-4]). Such a test setup is usually modelled as a two dimensional (2D) plane stress or plane strain system to reduce the computational cost.

However, concrete is a composite material with multiple phases including coarse aggregates, mortar and interfaces. Much of the existing numerical research on debonding failures in FRP-to-concrete interfaces has assumed concrete to be homogeneous and modelled the test set-ups as two dimensional (2D) plane stress or plane strain systems. This homogeneous 2D modelling method presents a number of limitations, as it ignores the 3D nature of the structure due to the spatial shape and distribution of coarse aggregates. Especially, when the simulation has to consider the heterogeneous nature of concrete, the plane stress or plane strain assumption is not valid for meso-scale models with coarse aggregates. For example, many existing mesoscopic researches simulate aggregate by numerous randomly computer generated polygons, what resembles aggregates as prisms in 2D meso-scale modelling. However in reality, the shape of aggregates is closer to a polyhedron. This means that in a 2D model, an aggregate of the maximum size occupies a much larger portion of cross section than in reality. Thus this characteristic element of the heterogeneity of concrete has a much greater influence on the specimen behaviour in a 2D model than in a 3D model [5].

This paper presents a comparative test between FRP-to-concrete and FRP-to-mortar bond using a bending test set up. Compared to concrete, mortar is a more uniform material so most of the 3D effects introduced by the coarse aggregates could be eliminated and at the same time, mortar shares a similar mechanical behaviour with concrete. By comparing the strain distribution across the width of the FRP plates, this work aims to investigate the 3D effect due to the presence of coarse aggregates on FRP-to-concrete bond behaviour.

EXPERIMENTAL TEST DESIGN

The beam test, in which usually two concrete blocks are linked by a hinge at the compression side and are strengthened by FRP plates at the tension side, is chosen as the test set-up. The modification recommended by Chen et al [6] was adopted for this test setup where the steel hinge at the compression side of the concrete blocks is replaced by two 12 mm diameter steel rebars, see Figure 1. The cube compressive strength (average of six 100 mm ×100 mm ×100 mm cubes) and the split tensile strength (average of five 200 mm ×100 mm diameter cylinders) of all of the concrete/mortar materials are shown in Table 1. The unidirectional carbon fibre sheet used in this experiment is the S&P C-Sheet 240 (300 g/m^2), with a guaranteed elastic modulus of 250 GPa, a guaranteed tensile strength of 4300 N/mm^2, a rupture elongation of 1.7%, and a nominal thickness of 0.168 mm. As recommended by the manufacturer, S&P Resin Epoxy 55, the solvent-free, transparent 2-component epoxy resin with a tensile strength of 35 MPa after 7 days, was used for the wet lay-up process.

Table 1. Material properties of concrete and mortar specimens

	FRP-concrete specimens		FRP-mortar specimens	
Properties	Concrete (test block)	Concrete (structural block)	Mortar (test block)	Concrete (structural block)
Compressive strength (MPa)	54.0	81.0	63.0	74.0
Tensile strength (MPa)	4.45	4.75	4.30	4.60

According to the bond strength model proposed by Chen & Teng [7], the effective bond length is

$$L_e = \sqrt{\frac{E_p t_p}{\sqrt{f_c'}}} \quad (1)$$

where E_p and t_p are the Young's modulus and the thickness of the FRP sheet, respectively, and f_c' represents the compressive strength of concrete cylinders. The design cylinder strength of the concrete specimen is 40 MPa, which leads to an effective bond length of 81.5 mm. A larger value than this was chosen to avoid the effect of the bond length. Thus concrete/mortar prisms of 298 mm × 150 mm × 100 mm was adopted the bending test.

As shown in Figure 2, a 409 mm long CFRP sheet which had the same width of the beam was bonded to the bottom of the two concrete blocks symmetrically, providing a bond length of 200 mm on both blocks. In order to ensure that the failure would only occur in the left (test) concrete block, the right block (referred as structural block) was cast with two longitudinal 12 mm tensile rebars and three 8 mm stirrups, and then strengthened with an additional layer of 100 mm long CFRP sheet bonded onto it. For the same reason, in both concrete and mortar test specimens, a higher design compressive strength was adopted for the structural block than that of the test block. The specimens were tested under 4-point bending, with a loading span of 100 mm.

SPECIMEN PREPARATION AND TEST PROCEDURE

A total of 6 test specimens were prepared, including 3 mortar-concrete (M-1 to M-3) and 3 concrete-concrete (C-1 to C-3) specimens. Each specimen consisted of two separate blocks, joined by 12 mm diameter steel reinforcement. Concrete was cast into the plywood formwork. A 9 mm wood plate wrapped in cling film was placed in the middle of the mould to create the gap between two blocks. The specimens were moved to the water tank after 24 hours. After 28 days of curing, the bottom surfaces of the specimens were treated using a handheld concrete grinder to expose the coarse aggregates (mortar blocks were ground to the same depth as the concrete blocks). Afterwards, compressed air was used to remove the dust. The carbon fabrics were cut to the designed size (Figure 2) using a knife and a ruler. Following a wet lay-up procedure, the carbon fabric was saturated thoroughly in the Resin Epoxy 55 bath and the roughened surfaces of concrete/mortar blocks were also saturated with resin. The saturated carbon fabrics were then placed on the concrete/mortar surface. Press roller and rubber spatula were used to smooth the sheets, distribute the laminating resin and remove air bubbles.

Six specimens were tested under 4-point bending test. The first specimen (M-3) was tested under 4-point bending test with a distance of 100 mm between the two point loads (loading span). However, the failure mode of this specimen was a shear crack induced debonding- a debonding originated at the

intersection of the shear crack and the CFRP and then propagated towards the beam's support. In an effort to avoid this failure mode, a loading span of 50 mm was adopted for the remaining 5 specimens.

The test was conducted on a Zwick machine with a load capacity of 100 kN. The test specimens were simply supported at both ends with a support span of 549 mm. Load was applied using a displacement control mode at a rate of 0.3 mm/min.

For each specimen, nine 6mm TML FLAB-6-11 strain gauges (SGs) were installed. Five of these SGs were installed longitudinally on the FRP sheet on the test side with the first one located beneath the edge of the test block, to measure the longitudinal FRP strain at locations as shown in Figure 3. The four remaining SGs were installed along the width of the FRP sheet at the same longitudinal location as the second strain gauge to measure the strain distribution across the width of the FRP. SGs were connected to a data logger which recorded the strain data every 0.5 seconds.

To ensure an accurate measurement of the net deflection at the mid-span, exclusive of the effects of the deflection of the testing fixtures and machine itself, a "Japanese Yoke" frame was attached to the neutral axis of the beams (Figure 5). A video-extensometer was used to measure the deflection of the beam by means of a virtual (contactless) gauge, which measures the relative displacement between the mid-span of the beam and a target point marked on the mid-length of the yoke.

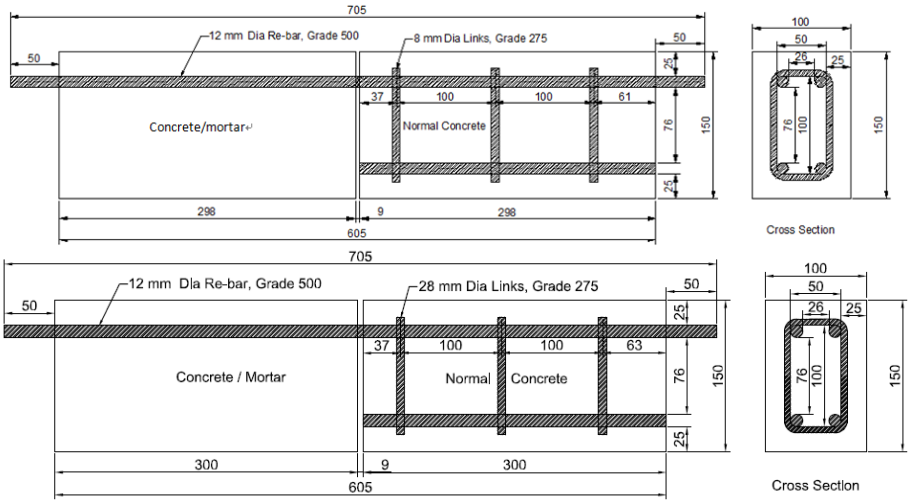

Figure 1. Details of the test specimens

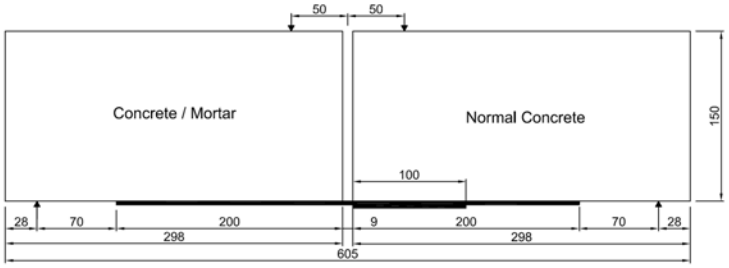

Figure 2. FRP geometry and support positions in the beam test

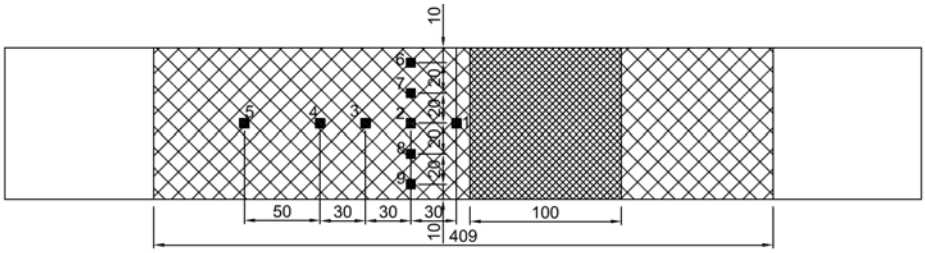

Figure 3. Location of the strain gauges

TEST RESULTS AND ANALYSIS

Load-Deflection Behaviour and Failure Process

The force versus mid-span deflection responses are shown in Figure 4. It can be seen that initially, the force response increases almost linearly as the deflection increases, and the initial slopes of different curves from the repeat tests are almost the same. A further increase in the deflection beyond this linear branch is accompanied with a reduction in the specimen's stiffness, indicating the initiation of micro-cracks. For all the three concrete beam-bending tests, and mortar beam-bending tests M-2 and M-3, the failure mode was the brittle CFRP debonding induced by the development of the shear crack near the mid-span of the beam (Figure 5), whereas for M-1, the failure mode was a brittle mortar block failure with a major crack initiated from the bonded end of the CFRP sheet and propagated towards the steel bars in the compression zone.

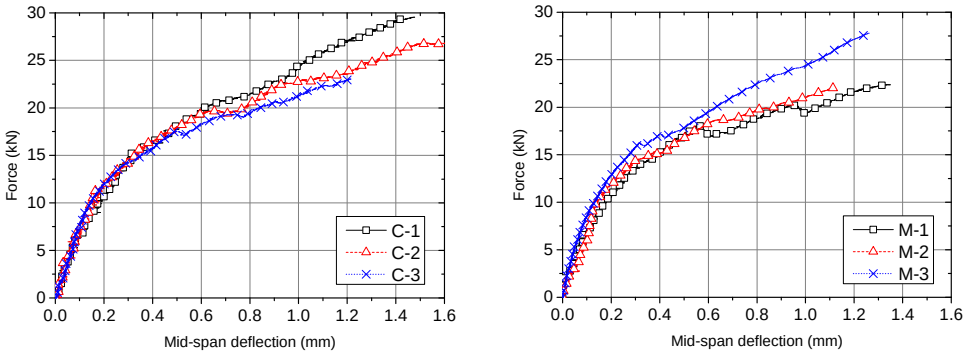

Figure 4. Force versus deflection response of concrete and mortar beam-bending tests

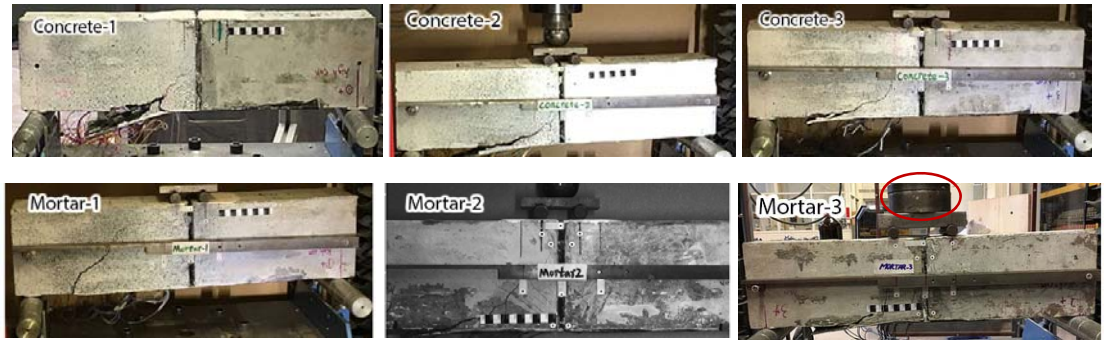

Figure 5. Failure modes of the test specimens

Development of FRP Strain

The full range strain history was measured by nine 6 mm SGs located as shown in Figure 3. The measurements were recorded every 0.5 s. The trends of strain measurements of the three concrete/mortar beam-bending tests are very similar, indicating a good repeatability of the test. Due to the page limit, only test results of one specimen in each group is presented here, in Figure 6 and Figure 7. SG1 to SG5 measure the strain distribution along the longitudinal direction of the CFRP sheet, whereas strain gauges SG2 and SG6 to SG9 measure the strain distribution across the width of the CFRP sheet. As expected, the strain development of the CFRP sheet started from the mid-span gap so the strain measurement of SG1 is greater than other SGs throughout the test. If concrete and mortar specimens were in elastic stage, the SG1 strain in the CFRP should be similar for a given applied load for both specimens. When the specimen starts to crack, the position of the crack would significantly affect the stress inside concrete/mortar specimens, as well as the strain in the CFRP. Figure 5 presents the final fracture mode of the specimens – the crack of C-1 initiated near the mid span of the specimen, whereas the M-1 failed at a shear crack starting from the bonded end of the CFRP sheet. It could be expected that the measurement of SG1 in C-1 would be higher than that of the M-1.

For the concrete specimen, at the same longitudinal position, there is a notable difference between the measurements of SG2 and SG6 to SG9. This indicates that the non-uniformity of the concrete attached

to the CFRP sheet would result in a non-regular mechanical response of the FRP-to-concrete bonded joint. For the mortar beam specimen, the difference of the strain measurements across the width direction is much smaller than that of the concrete beams, and the strain measurements show an obvious similar trend. This will be further analysed and discussed quantitatively in the next section.

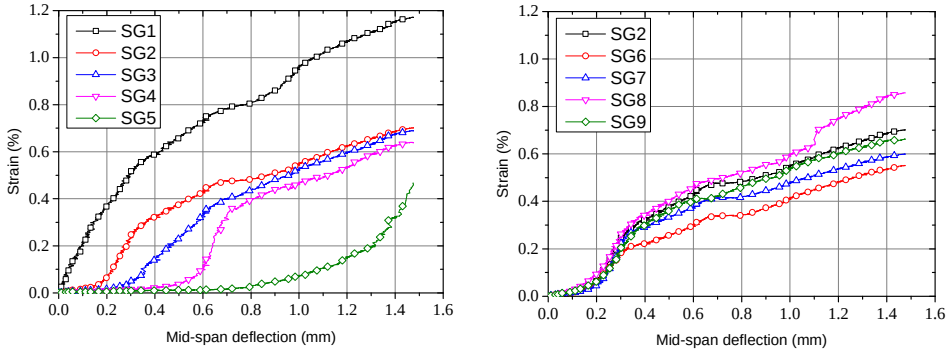

Figure 6. Strain-deflection relationship of concrete beam bending test C-1

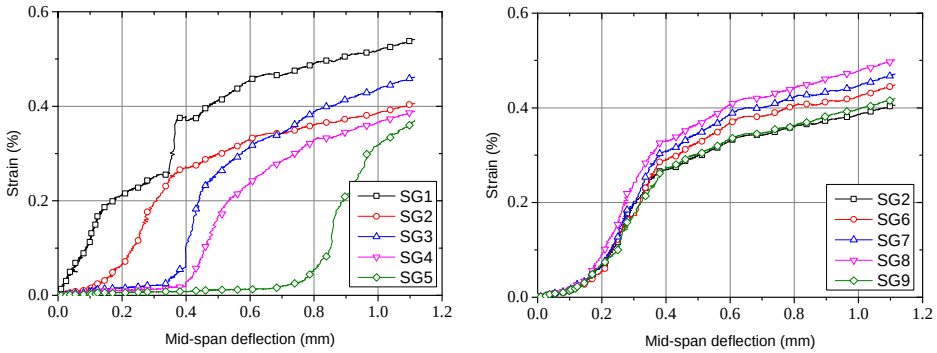

Figure 7. Strain-deflection relationship of mortar beam bending test M-2

Strain Distribution across the FRP Width

Figure 8 and Figure 9 show the distributions of strain in the CFRP sheet across the width at different load levels for a concrete and a mortar specimen (C-1 and M-2), respectively. The load level is defined as the percentage of the current load over the ultimate load. Figure 8a and Figure 9a show the strain profile at load levels ranging from 10% to 100%. It can be seen that the strain distribution in the concrete specimen is generally more scattered than that in mortar specimen. This phenomenon is more obvious at lower load levels (see Figure 8b and Figure 9b) where the test specimen was almost elastic, without the effect of macro cracking.

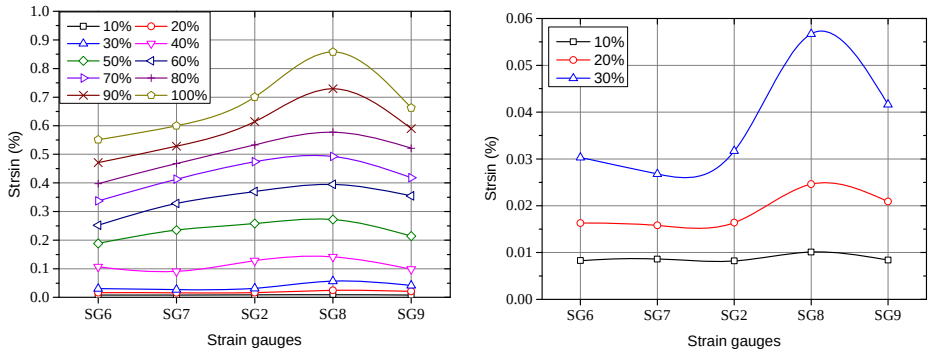

(a) All load levels (b) Lower load levels

Figure 8. FRP strain distribution across the FRP width at different load level in FRP-to-concrete bond specimen C-1

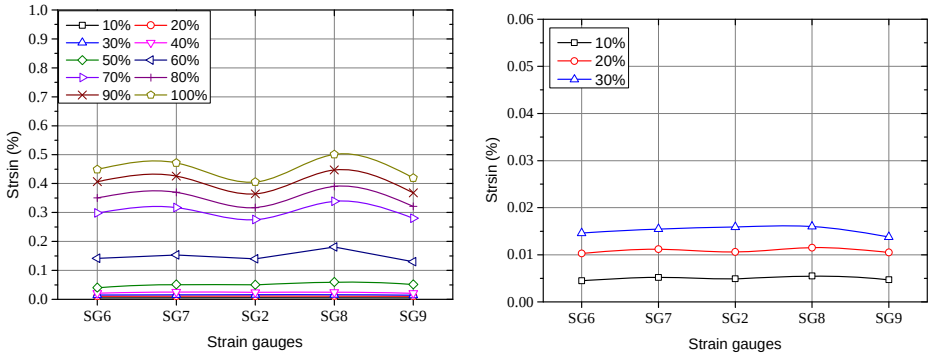

(a) All load levels (b) Lower load levels

Figure 9. FRP strain distribution across the FRP width at different load level in FRP-to-mortar bond specimen M-2

In order to quantify the scatter of the strain distributions, their variation is analysed through the coefficient of variation (CoV). The CoV is defined as the ratio of the standard deviation to the mean value. From the strain distribution at each load level, the average strain and its corresponding CoV can be calculated.

Table 2 summaries the CoV of strain distribution at different loading levels at a 10% interval. The variation of the strain distribution across the width of the FRP in the concrete specimen is consistently higher than that of the mortar specimen throughout the loading process. The average variation (CoV) in the concrete specimen C-1 is about two times of that in the mortar specimen M-2.

Table 2. The CoV of strain distribution at different loading level

Loading level	FRP-Concrete specimen C-1	FRP-mortar specimen M-2
10%	9.1%	6.8%
20%	20.4%	4.7%
30%	32.3%	6.2%
40%	19.6%	7.6%
50%	14.2%	13.4%
60%	16.1%	13.2%
70%	14.3%	8.7%
80%	13.8%	8.9%
90%	16.5%	8.9%
100%	17.4%	8.6%
Average	17.4%	8.7%

CONCLUSIONS

This paper has presented an experimental test programme on the strain distribution in FRP in both FRP-to-concrete and FRP-to-mortar bonded joints using a bending test setup. The aim of the study was to investigate the effect of coarse aggregates in concrete on the strain distribution across the width of the FRP. A total of six specimens were tested: three concrete and three mortar. The test results confirmed that the presence of coarse aggregates results in a remarkable variation in the FRP strain distribution across the width of the FRP. This variation is about two times higher in a FRP-to-concrete bonded joint than that in a FRP-to-mortar bonded joint.

ACKNOWLEDGEMENT

The first author is grateful for the scholarship provided by the China Scholarship Council (CSC). The authors would like to express their gratitude to “S&P Clever Reinforcement Company AG” and in particular its senior structural engineer Mr Martin Hüppi for supplying the CFRP materials. They would also like to acknowledge that Mr Weilun Ding participated in the experimental work.

REFERENCES

1. Teng, J. G., Chen, J. F., Smith, S. T. and Lam, T., *FRP-strengthened RC structures*, Chichester, Wiley, (2002).
2. Ali-Ahmad, M., Subramaniam, K. and Ghosn, M., Experimental investigation and fracture analysis of debonding between concrete and FRP sheets, *Journal of Engineering Mechanics*, **132(9)**, 914–923 (2006).
3. Yao, J., Teng, J. G. and Chen, J. F., Experimental study on FRP-to-concrete bonded joints, *Composites Part B: Engineering*, **36(2)**, 99–113 (2005).
4. Wu, Z. S., Yuan, H., Hiroyuki, Y. and Toshiyuku, K. , Experimental/analytical study on interfacial fracture energy and fracture propagation along FRP-concrete interface, *ACI International*, **SP-201(8)**, 133–152 (2001).
5. Vonk, R. A., Micromechanical investigation of softening of concrete loaded in compression, *Heron*, **38(3)**, 5–94 (1993).
6. Chen, J. F., Li, X. Q., Lu, Y., May, I. M., Stratford, T. J., O'Sullivan, R. and Sheil, A., A new test method for FRP-to-concrete bond behaviour under impact loading, *The 12th International Symposium on Structural Engineering*, Wuhan, China, November 17, 2012.
7. Chen, J. F. and Teng, J. G., Anchorage strength models for FRP and steel plates bonded to concrete, *Journal of Structural Engineering*, **127 (7)**, 784–791 (2001).